J Nanopart Res (2014) 16:2415
DOI 10.1007/s11051-014-2415-1

RESEARCH PAPER

Raman spectroscopy for probing covalent functionalization of single-wall carbon nanotubes bundles with gold nanoparticles

Larissa Otubo · Odair Pastor Ferreira · Antonio Gomes Souza Filho · Oswaldo Luiz Alves

Received: 28 December 2013 / Accepted: 9 April 2014 / Published online: 27 April 2014

Abstract A hybrid system made of single-wall carbon nanotube bundles (average diameter of approximately 20 nm and length of several tens of nanometers) highly covered with gold nanoparticles (average diameter of 5 nm) was prepared through the functionalization of the nanotube surface with 4,4′-thiobisbenzenethiol molecules followed by the anchoring of gold nanoparticles. The decoration of single wall carbon nanotubes with gold nanoparticles was performed using two different methods, named as *ex situ* and in situ, which refer to the gold reduction before or during the contact with the nanotubes, respectively. Transmission electron microscopy images showed that both methods lead to a successful decoration of the single wall carbon nanotube bundles, although different density of gold nanoparticles covering the bundles was observed to depend on the reaction methods. Resonance Raman spectroscopy data were used to follow the electronic changes of the carbon nanotubes after gold nanoparticles loading and confirmed the strong interactions of the gold nanoparticles with the 4,4′-thiobisbenzenethiol molecules and the carbon nanotubes. This interaction was probed in the Raman spectrum which unveiled a surface enhancement Raman effect of the thiol molecule Raman signals, not observed before the attachment of metallic nanoparticles onto 4,4′-thiobisbenzenethiol functionalized carbon nanotubes.

Keywords Carbon nanotubes · 4,4′-Thiobisbenzenethiol · Surface enhancement Raman spectroscopy · Functionalization · Hybrid nanosystems

L. Otubo (✉) · O. L. Alves (✉)
LQES – Laboratório de Química do Estado Sólido, Institute of Chemistry, University of Campinas (UNICAMP), P.O. Box 6154, Campinas, SP 13083-970, Brazil
e-mail: larissa.otubo@ipen.br

O. L. Alves
e-mail: oalves@iqm.unicamp.br

L. Otubo
Centro de Ciência e Tecnologia de Materiais, Nuclear and Energy Research Institute (IPEN), Av. Prof. Lineu Prestes, 2242 - Cidade Universitária, São Paulo, SP 05508-000, Brazil

O. P. Ferreira
LaMFA – Laboratório de Materiais Funcionais Avançados, Departamento de Física, Universidade Federal do Ceará, P.O. Box 6030, Fortaleza 60455-900, Brazil

A. G. S. Filho
Departamento de Física, Universidade Federal do Ceará, P.O. Box 6030, Fortaleza, Ceará 60455-900, Brazil

Introduction

The hybrid nanosystems obtained by combining 1D and 0D nanomaterials are very interesting systems because they exhibit synergistic properties which are

either new or improved as compared with their isolated counterparts. Single wall carbon nanotubes (SWCNTs) are special supporters for metallic nanoparticles because their electronic structure is extremely sensitive to changes in the environment such as chemical processes occurring at the surface of the nanoparticle. SWCNTs decorated with metallic nanoparticles are one of the most studied and promising hybrid materials owing to their remarkable optical, electronic, and mechanical properties along with the rich chemistry and functionality of metallic nanoparticles, which are potential systems for applications in catalysis and sensor devices (Star et al. 2006; Kim and Mitani 2006; Mubeen et al. 2007; Suni 2008; Wu et al. 2009; Zhu et al. 2009; Kauffman et al. 2010).

Different strategies have been used to obtain the abovementioned hybrid materials. Since pristine carbon nanotubes are chemically inert, the efficient anchoring of nanoparticles onto their surface demands some previous chemical modification of the nanotube wall aiming to promote a better interaction with the particles (Hirsch 2002; Balasubramanian and Burghard 2005; Ramanathan et al. 2005; de Souza Filho and Fagan 2007). This process is needed for improving both anchoring strength and increasing the loading amount (Hirsch 2002; Ellis et al. 2003; Jiang and Gao 2003; Balasubramanian and Burghard 2005; Ramanathan et al. 2005; de Souza Filho and Fagan 2007). In this scenario, both covalent (Lim et al. 2003; Kim et al. 2006; Raghuveer et al. 2006; Zanella et al. 2006; Voggu et al. 2008; Hou et al. 2009) and non-covalent (Liu et al. 2003; Chen et al. 2007; Scolari et al. 2008; Zhang et al. 2009) functionalizations of carbon nanotubes with chemical species with high affinity toward metallic nanoparticles are desired.

The non-covalent functionalization is interesting if one desire to preserve the electronic properties of the carbon nanotubes. The electrodeposition technique has been used to decorate SWCNTs with Ag, Au, Pt, and Rh nanoparticles with sizes varying from 30 to 300 nm. These systems were used in Surface-enhanced Raman spectroscopy (SERS) studies of carbon nanotubes (Chen et al. 2007; Scolari et al. 2008) as well as sensors for CO and NO detection (Kauffman and Star 2007; Kauffman et al. 2010). Liu et al. (2003), and Ou and Huang (2006) used bifunctionalized molecules to bridge gold nanoparticles (AuNPs) with carbon nanotubes, having at one end, groups like –SH or $–NH_2$ to interact with the AuNPs, and at the other, a pyrenil group used to interact with the nanotube surface through π–π interaction. Ionic surfactants have also been used to promote the interaction of carbon nanotubes with electrically charged metallic nanoparticles through electrostatic forces (Jiang et al. 2003; Jiang and Gao 2003; Zhao et al. 2008).

The covalent modification of the carbon nanotube uses the defects present in the nanotubes wall to promote some chemical reactions and addition of functional groups on their surface, which allow a strong interaction with metallic nanoparticles. These defects could be generated through oxidative treatment and the use of organic molecules with high affinity toward metallic nanoparticles, such as thiols and amines (Lim et al. 2003; Hu et al. 2005; Kim et al. 2006). Srivastava et al. (2013) used natural organosulfurs from *Allium sativum* (garlic) to modify MWCNTs and promote their interaction with gold nanoparticles (AuNPs). By using a crosslinker, Kumar et al. (2012) covalently bonded 4-aminothiophenol functionalized AuNPs to carboxilated MWCNTs.

In another hand, the detailed study of the interaction of carbon nanotube and nanoparticles is challenging. Among different techniques, Raman spectroscopy is a very sensitive tool used for monitoring the functionalization of carbon nanotubes, because this process can be probed in both D (disorder band) and G band (graphitic band). Furthermore, the interaction with metal nanoparticles could modify the electronic structure of the SWCNTs observed by changes in the G and radial breathing modes (RBM) bands, as showed by Voggu et al. (2008) by comparing SWCNTs coated with gold and platinum nanoparticles prepared with microwave treatment without previous functionalization and AuNP covalently linked to SWCNTs by click reaction. The Raman spectra of those samples showed an increase in the proportion of the metallic SWCNTs species on interaction with metallic nanoparticles. Their ab initio calculations showed that such interactions between the metal atoms and SWCNTs modify the electronic structure of the tubes rendering them metallic, i.e., the anchoring of metal nanoparticles induces a semiconductor to metal transition in SWCNTs.

In this paper, the interaction between SWCNTs bundles (average diameter of approximately 20 nm and length of several tens of nanometers) and AuNPs was intermediated by 4,4′-thiobisbenzenethiol (TIOB)

which is an electron delocalized π-system (Weckenmann et al. 2002; Li et al. 2003). The linkage between 1D (nanotubes) and 0D (gold nanoparticles) materials was made via an aromatic organothiol molecule, which is used not only for promoting a uniform distribution of gold nanoparticles, but also for exploiting the delocalized π electrons as efficient mediators of charge transfer process between the metal nanoparticle and nanotubes. SWCNTs were firstly functionalized with these oligophenylthiol molecules prior to anchoring of AuNPs. The syntheses of the hybrid systems were performed using two methods named here as *ex situ* and in situ. The *ex situ* method consists in preparing the gold nanoparticles separately and then promotes the interaction with nanotubes in a second step. The in situ method consists of synthesizing the AuNPs in the presence of functionalized carbon nanotubes. The characterization of the systems using different techniques revealed that the functionalization of SWCNTs with the oligophenylthiol has a strong affinity to AuNPs, thus leading to a regular coverage of the SWCNT surface with the AuNPs. Resonance Raman spectroscopy data were used for studying the charge transfer process between the AuNPs and SWCNTs mediated by TIOB (Liu et al. 2001; Weckenmann et al. 2002). Surface-enhanced Raman effect (SERS) due to AuNPs coverage allowed us to observe the Raman signal of the 4,4′-thiobisbenzenethiol molecules which are functionalizing the SWCNTs, thus providing detailed information about the interaction between AuNPs and the chemical linker bonded to the carbon nanotube surface.

Experimental

Materials

Single wall carbon nanotubes (SWCNTs, as-prepared, synthesized by arc discharge) were purchased from Carbolex Inc. The chemicals 4,4′-thiobisbenzenethiol, tetraoctylammonium bromide, tetrachloroauric(III) acid, and sodium borohydride were purchased from Aldrich and were used as received. Thionyl chloride was distilled before usage.

SWCNT purification

The purification process was carried out following the method described by Furtado et al. (2004). The nanotubes were thermally treated at 360 °C for 90 min, under synthetic air flow, followed by reflux in 3 mol L^{-1} nitric acid solution for 16 h. After the reflux treatment, the suspension was filtered using a polycarbonate membrane (0.2 μm porosity) under vacuum. The solid was washed several times with hot deionized water until reaching pH 5. Afterwards, a NaOH solution (pH 10) was added, and the solid was rinsed with hot deionized water until reaching pH 7. The solid was dried under vacuum conditions for 2 h and named as SWCNT-COOH.

Functionalization of SWCNTs with 4,4′-thiobisbenzenethiol

The method used to attach the thiol groups to the SWCNT surface has two steps: (i) formation of acid chloride groups and (ii) reaction with dithiol molecules of 4,4′-thiobisbenzenethiol (TIOB) (Peng et al. 2003; Kim et al. 2006).

In a typical synthesis, 20 mg of oxidized SWCNTs (SWCNT-COOH) were added to 10 mL of freshly distilled thionyl chloride. The suspension was sonicated for 6 h and then refluxed for 12 h under argon atmosphere. The thionyl chloride excess was evaporated under argon. Then 10 mL of a 0.05 mol L^{-1} 4,4́-thiobisbenzenthiol solution in toluene was added to the solid. The suspension was sonicated for 6 h followed by reflux treatment for 18 h. The product, named as SWCNT-SH, was filtered using a PTFE membrane (0.2 μm porosity) and rinsed with toluene and ethanol to remove the excess of residual dithiol. The solid was dried under vacuum conditions. See the schematic representation of this functionalization in Fig. 1.

Gold nanoparticle loading on SWCNTs

The gold nanoparticles (AuNPs) and carbon nanotube interactions were performed using two methods, named here as in situ and *ex situ*. Both methods used a gold starting solution prepared by stirring a $HAuCl_4$ aqueous solution with a tetraoctylammonium bromide (TOAB) solution in toluene. A 4.4:1 molar ratio of TOAB:Au was used. The resulting organic phase containing $[AuCl_4]^-TOA^+$ (9.85×10^{-3} mol L^{-1}) was separated and used as the gold starting solution.

The reactions were performed using 2 mg of SWCNT-SH. The thiol content, 1.73×10^{-6} mol in

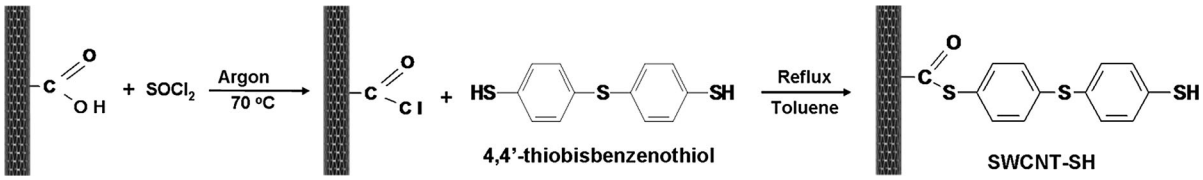

Fig. 1 Schematic representation of functionalization reactions of SWCNTs with dithiol molecules

2 mg of SWCNT-SH, was estimated by energy dispersive X-ray spectroscopy (EDS). Based on this estimation, the reactions were performed by using different Au:thiol molar ratios: 1:2 ($n_{Au} = 8.6 \times 10^{-7}$ mol), 4:1 ($n_{Au} = 6.9 \times 10^{-6}$ mol), 6:1 ($n_{Au} = 1.0 \times 10^{-5}$ mol).

AuNPs loading on SWCNTs using the *ex situ* method

In a typical *ex situ* preparation of AuNPs, a $[AuCl_4]^-TOA^+$ solution in toluene was placed in a 25-mL round bottomed flask containing a $[AuCl_4]^-$ quantity of interest for each Au:thiol ratio used, as described previously. 1.0 mL of a freshly prepared $NaBH_4$ aqueous solution was added to the reaction under vigorous stirring ($NaBH_4$:Au molar ratio of 11:1). After stirring for 2 h, 2 mg of carbon nanotubes were added. The suspension was sonicated for 0.5 h, followed by stirring for 1.5 h. The solid was isolated by filtration using a PTFE membrane (0.2 μm pore). The product was rinsed with several portions of toluene, ethanol, and deionized water. The solid was dried under vacuum conditions. The samples prepared by this method were named as SWCNT-Au-E-12 and SWCNT-Au-E-41, which correspond to Au:thiol molar ratios of 1:2 and 4:1, respectively.

AuNPs loading on SWCNTs using the in situ method

In a typical in situ preparation of AuNPs, 2 mg of carbon nanotubes were added into a 25-mL round bottomed flask and dispersed in a $[AuCl_4]^-$ TOA^+ solution in toluene containing the $[AuCl_4]^-$ quantity of interest for each Au:thiol molar ratio. The suspension was sonicated for 0.5 h, and then, under stirring, 1.0 mL of a freshly prepared aqueous $NaBH_4$ solution (in a $NaBH_4$:Au molar ratio of 11:1) was added. The suspension was stirred for 2 h and filtered using a PTFE membrane (0.2 μm pore). The product was rinsed by several portions of toluene, ethanol, and deionized water. The solid was dried under vacuum conditions. The samples prepared by this method were named as SWCNT-Au-I-12, SWCNT-Au-I-41, and SWCNT-Au-I-61, which correspond to Au:thiol molar ratios of 1:2, 4:1, and 6:1, respectively.

Experimental techniques

UV–visible (UV–Vis) absorption experiments were carried out in a Hewlett Packard spectrophotometer, model 8452A. Transmission electron microscopy (TEM) images and energy dispersive spectroscopy (EDS) analysis were obtained using a JEOL JEM-3010 (300 kV) microscope coupled with an EDS detector and a JEOL JEM 2100 (200 kV) with a scanning TEM (STEM) unit and an EDS detector. The TEM samples were prepared by dropping isopropanol sample suspensions on a holey carbon film on a 400 mesh copper grid and letting the solvent evaporate at room temperature. Raman spectra were recorded on a Renishaw system 3000 Raman imaging microscope (ca. 1 μm spatial resolution) using a He–Ne laser (1.96 eV) and Ar^+ ion laser (2.41 eV). The laser power density was optimized in order to avoid overheating of nanotube samples by the laser beam. Dynamic light scattering (DLS) measurements were carried out in a Malvern Instruments Zetasizer, model Nano-ZS, using a He–Ne laser.

Results and discussion

Functionalization of SWCNTs with thiol groups

The chemical modification of the SWCNTs started with the purification process which aims to eliminate the amorphous and the graphitic carbon particles and to decrease the remaining catalyst metal content on the

sample. This process also adds oxidized functional groups such as –COOH and –OH to the nanotube surface, among others. These sites can be further used as starting points to anchor other chemical species. These oxidized SWCNTs were treated with thionyl chloride to form acid chloride groups on the nanotube surface. Such chemical groups are highly reactive in the presence of water, alcohols, thiols, and amines. Therefore, in order to minimize parallel hydrolyses, the reaction with the dithiol (4,4′-thiobisbenzenethiol) were carried out under inert and dry atmosphere, using toluene as a solvent. The scheme of the SWCNTs functionalization reactions is shown in Fig. 1.

The resonance Raman spectra of the thermally treated, HNO_3-treated SWCNTs and thiol-functionalized SWCNTs excited with $E_{laser} = 1.96$ eV are shown in Fig. 2. For thermally treated SWCNTs we can identify the radial breathing modes (RBM) at low frequency range, which are typical of these nanotubes. The G band profile (lower spectrum) is characteristic of metallic nanotubes, thus indicating that 1.96 eV laser energy is in resonance with the first electronic transitions of metallic carbon nanotubes. The disorder-induced mode (D band) is also observed at about 1,250 cm^{-1}, and its relatively low intensity indicates a low number of defects in the thermally treated SWCNTs. After the HNO_3 treatment (SWCNT-COOH sample), the RBM intensity decreases. The intensity of this mode is strongly dependent on the electronic changes of the carbon nanotubes, which in turn affects the resonance conditions. The anchoring of some groups to the tube surface also affects the totally symmetric vibrations, thus explaining their spectral broadening and reduced intensity. The acid treatment leads to an increase in the D/G intensity ratio along with a change in the G band profile (see middle spectrum). The D/G intensity ratio increased after the carboxylation, thus unveiling an increase in the disorder degree of the SWCNTs surface due to a covalent functionalization of nanotubes with carboxylic and hydroxyl groups. The observed change in G band profile is attributed to changes in the electronic properties of the nanotubes through charge transfer processes. The decrease in the intensity of the G band component with lower wavenumber (the so called G^- band marked with arrow in Fig. 2a) indicates a decrease in the metallic character of the resonant nanotubes in the sample, and its frequency shift is attributed to electron transfer from the SWCNTs through the oxidation process (Kim et al. 2005). A similar frequency upshift was observed in the second-order G′ band observed at about 2,630 cm^{-1} (see the middle spectrum in Fig. 2b).

The Raman spectrum of the SWCNTs modified with the dithiol molecules (SWCNT-SH) is shown in the upper spectrum of Fig. 2a and b. The G band profile changed upon functionalization with the dithiol groups, whereby a decrease in the G^- intensity relative to G^+ band (the higher wavenumber component of G band) intensity was observed. This effect is associated with the downshift of Fermi level of the metallic carbon nanotubes as a consequence of a charge transfer process from the tubes to the dithiol molecules. It is well known that the G^- band for the metallic carbon nanotubes exhibit the broad profile (called Breit–Wigner–Fano) due to the strong coupling of phonons with the electrons at the Fermi level. When the Fermi level is downshifted by charge transfer from the nanotubes to the functional molecules, this coupling decreases the band intensity and the asymmetric profile changes to a more symmetrical profile (Fagan et al. 2005; Costa et al. 2009; Li et al. 2013) The origin of this phenomena is based on the so called Kohn anomaly which renormalize the phonon frequency and linewidths as described in the literature.

The second-order G′ Raman band also carries information about functionalization of the nanotubes, because this mode is very sensitive to charge transfer effects. Both the shape and peak frequency of the second-order G′ band profile was affected by the carboxylation and dithiol bonding, as shown in Fig. 2b. The carboxylation induces a splitting of the G′ band of pristine SWCNT into two peaks as can be observed by the shoulder marked with up-arrow. The second peak in the G′ band spectra of nanotubes have been reported by Maciel et al.(2008), and it was explained by the presence of localized charge defects. According to their model, the new G'_D peak (defect-related) is associated with localized defects, such as a covalent bond, and appears at a higher frequency for SWCNTs doped with holes (the so called *p* doping) and at a lower frequency for SWCNTs doped with electrons (the so-called *n* doping). The upper component peak observed in the G′ spectra for both carboxylated and thiolated SWCNT is believed to originate from the regions localized near the sp^3-like

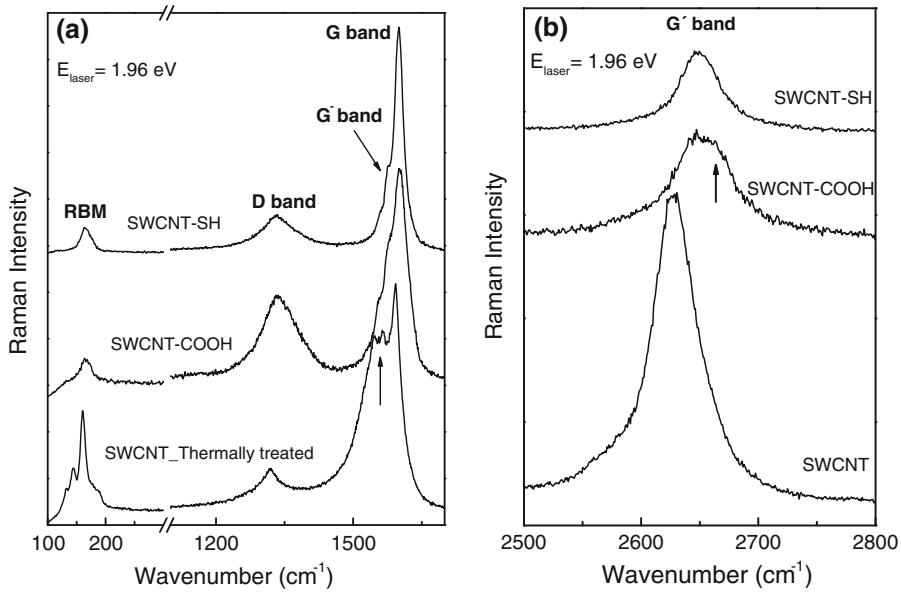

Fig. 2 Raman spectra in the **a** RBM, D-, and G-band and **b** G′-band regions for SWCNT thermally treated, SWCNT-COOH and SWCNT-SH using $E_{laser} = 1.96$ eV as excitation energy

carbon atoms which anchors –COOH and –CO-TIOB species. The peak labeled G'_D suggests that the SWCNT are losing electrons to these chemical groups. This result is consistent with the changes in the G band profiles (Fig. 2a), which changes from a metallic-like shape to a semiconductor-like shape as a consequence of Fermi level shift. The splitting of the G′ band is about 19 cm^{-1} which is comparable with values observed for boron-doped nanotubes (Maciel et al. 2008), a typical *p*-doped system.

The thiol peaks in the 4,4′-thiobisbenzenethiol Raman spectrum are expected to be observed at 738, 913, 1,075, and 2,555 cm^{-1} assigned to ν_{as}(C–S–C), δ(C–S–H), ν(C–S) and ν(S–H) vibrations, respectively (Wang et al. 2008). However, after the functionalization with the dithiol molecules, no characteristic bands of 4,4′-thiobisbenzenethiol were observed in the Raman spectrum, probably due to very high intensity of the nanotube Raman bands, which comes from a strong resonance Raman effect.

In order to further verify the thiol functionalization of the SWCNTs, the sample was analyzed by EDS coupled to the HRTEM. In Fig. 3, we show the integrated signal of SWCNTs obtained from the sample region highlighted in the inset (Fig. 3). The presence of sulfur atoms indicates that the functionalization of SWCNTs with dithiol molecule was successfully performed.

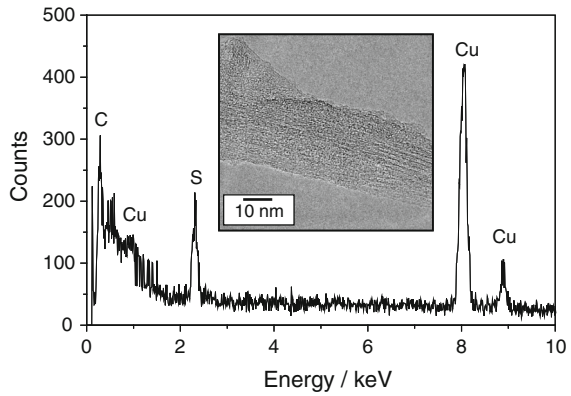

Fig. 3 EDS spectrum of SWCNT-SH corresponding to the TEM image showed in the *inset*. The Cu peaks observed on the spectrum are referred to the TEM copper grid used

Au nanoparticle loading on carbon nanotubes

The AuNPs loading on carbon nanotubes were performed using the thiol-functionalized SWCNTs (SWCNT-SH) as substrates using in situ and *ex situ* methods as outlined in Fig. 4 and described in the experimental section.

The UV–Vis absorption spectrum (Fig. 5) of the AuNPs dispersion before the interaction with carbon nanotubes (*ex situ* method) shows an absorption band at 535 nm, which is assigned to the surface plasmon band, thus indicating the formation of AuNPs. The

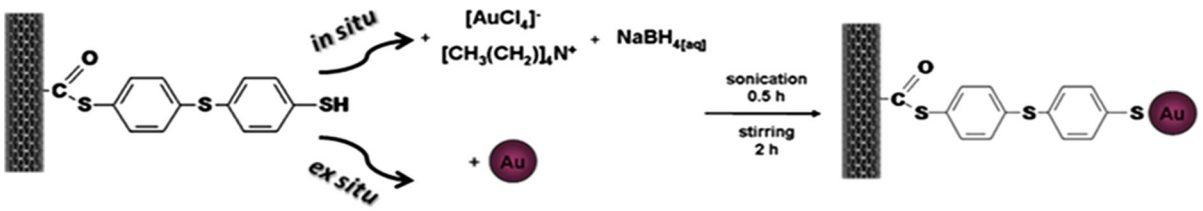

Fig. 4 Scheme of the in situ and *ex situ* methods for anchoring gold nanoparticles on SWCNTs

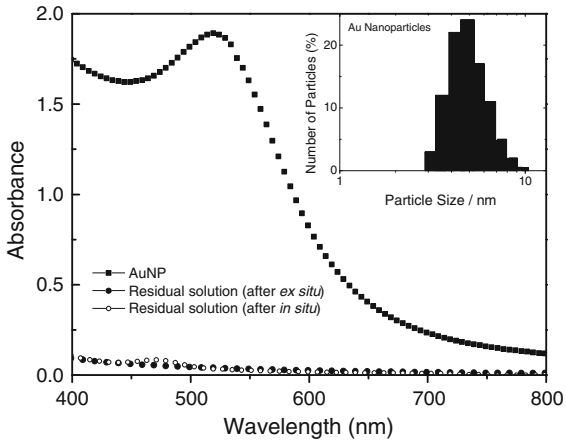

Fig. 5 UV–Vis absorption spectra of the AuNPs dispersion before (*solid squares*) and after (*solid circles*) *ex situ* interaction with SWCNT-SH. The *open circles* show the UV–Vis absorption spectrum of residual solution of AuNPs after in situ interaction with SWCNT-SH. The histogram of the AuNPs dispersion (*solid squares* spectrum) is shown in the *inset*

plasmon absorption band is very sensitive to changes in composition, size, and shape of the nanoparticle, as well as to the inter-particle distance (Liz-Marzán 2004). The AuNPs dispersion was characterized by the dynamic light scattering (DLS) technique, and the nanoparticle size distribution is shown in the inset to Fig. 5. The nanoparticle average size is about 5 nm, and 90 % of the AuNPs have diameters below 6.5 nm. After the interaction of the AuNPs with the SWCNT-SH, the solid was filtered. The UV–Vis absorption spectrum of the residual dispersion is shown in Fig. 5 as solid circles, and we notice that surface plasmon band absorption is absent, thus indicating that all the AuNPs in the dispersion were successfully loaded onto the SWCNT-SH surface. For comparison, we also show in Fig. 5 the UV–Vis absorption spectrum of the residual dispersion (open circles) used in the in situ reactions. No surface plasmon band absorption was observed, thus suggesting that this method also leads to a high yield of AuNPs loaded to the SWCNTs surface.

Resonance Raman spectra of AuNPs loaded on thiolated SWCNTs using 1.96 and 2.41 eV laser excitation energies are shown in Figs. 6 and 7, respectively. We show the Raman spectra for the AuNPs loaded SWCNTs prepared using both *ex situ* and in situ conditions with different Au:thiol molar ratios. It is important to mention that the 1.96 eV laser excites metallic nanotubes while 2.41 eV excites semiconducting nanotubes. The interaction of the AuNPs with the nanotubes also causes changes in the thiolated SWCNTs Raman bands. As observed in Fig. 6a, after AuNPs loading, we observed a broadening of the G band for both samples prepared using *ex situ* (E) and in situ (I) conditions that are caused by an increase in the G^- band intensity and linewidth, which indicates an increase in the metallic character of the nanotubes due to charge transfer from the AuNP to the thiolated SWCNTs (Voggu et al. 2008). The aromatic thiol molecules play an important role in this process. The in situ reactions lead to broader bands, indicating a stronger charge transfer process between AuNPs and SWCNTs. By analyzing the G′ band peak (Fig. 6), we observed that after decorating the carbon nanotubes with AuNPs, the wavenumber of this mode for samples prepared using the *ex situ* condition is slightly downshifted compared with the thiolated SWCNT. For samples prepared using in situ method, the G′ wavenumber does not change. Such differences are related to the different adsorption mechanisms of the nanoparticles, which in turn affect the electronic structure of the nanotubes in a different way.

In addition, the Raman spectra obtained using 2.41 eV laser energy (Fig. 7) also showed an upshift for both G and G′ band frequency of the carbon nanotubes after functionalization with 4,4′-thiobisbenzenethiol (SWNT-SH). This result indicates that a similar charge transfer process happens for metallic

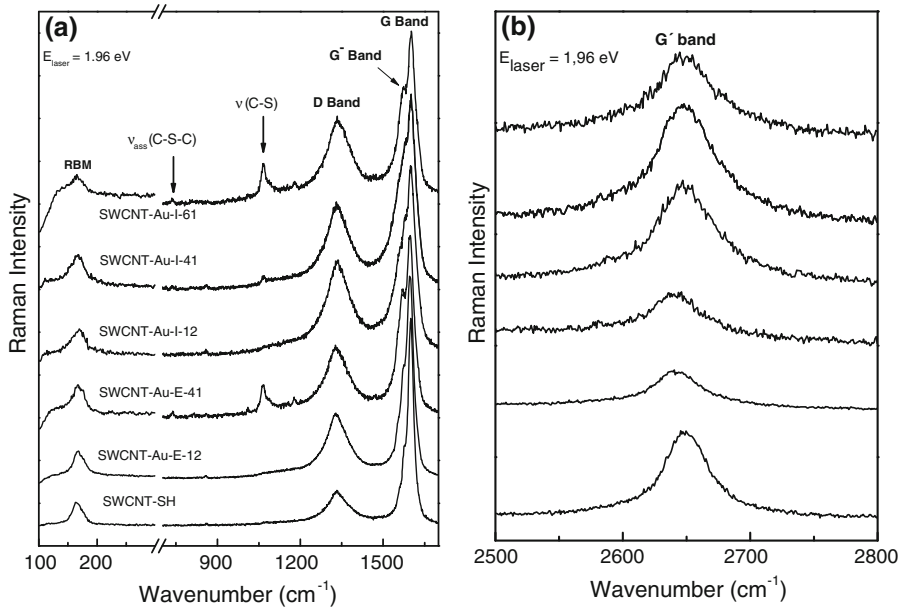

Fig. 6 Raman spectra in the **a** RBM, D- and G-band and **b** G′-band regions for SWCNT-SH, SWCNT-Au-E, and SWCNT-Au-I using 1.96 eV as excitation energy

and semiconducting nanotubes. The G band profiles of metallic carbon nanotubes are more affected because for these nanotubes there are electrons populating the Fermi level. Small changes in the Fermi level are enough for coupling phonons and electrons in the Fermi level through the Kohn anomaly effect, which in turns affect the G band profile as previously described (Farhat et al. 2007). A slight change in the G band profile is observed after interaction with AuNPs (in situ condition—SWNT-Au-41 and SWNT-Au-61). This upshift corroborates with the results observed for the metallic nanotubes, and can be interpreted as a transfer of electronic density from the semiconducting nanotubes to 4,4′-thiobisbenzenethiol molecules and weak charge transfer to nanotubes after AuNPs interaction. The G band profile changes are not so strong because the semiconductor nanotubes are not so sensitive to electronic changes as the metallic ones. It should be pointed out that quantifying the shift of the Fermi level due to the loading of AuNPs by using the changes observed in the G band is difficult here because the electron phonon coupling depends on the tube diameter and chirality, and the response we observed in the spectra of a bundle samples is an average over many tubes, and this kind of analysis is more appropriated for measurements on isolated tubes (Farhat et al. 2007). Another difficulty for quantifying the shift is that we do not know for sure what is the position of Fermi level for the unfunctionalized samples, because the post-synthesis processing can dope the nanotubes and move the Fermi level from neutrality point. Therefore, the presented results allow us to get only a qualitative description of the effects rather than a quantification of the changes in the Fermi level.

By examining the Raman spectra ($E_{laser} = 1.96$ eV, Fig. 6) of AuNP-loaded SWCNTs in the 700–1,200 cm^{-1} region, we observed new peaks (marked with down-arrows) for some of the samples. The peaks observed at 738 and 1,065 cm^{-1} are assigned to ν_{as}(C–S–C) and ν(C–S) vibrations, respectively, and the thiol peaks related to S–H bond vibrations were not observed (Wang et al. 2006). The intensity enhancement depends on the Au:thiol ratio as well as on the synthesis (in situ or *ex situ*) route. The observation of the Raman bands of thiol molecules is interesting on its own, because we can use this molecule as a probe for the interaction of the AuNPs through anchoring. The observation of the C–S–C and C–S modes is interpreted as being related to the surface-enhanced Raman scattering (SERS) effect (Kneipp et al. 1999; Wang et al. 2008), due to the presence of the AuNPs covering the dithiol-functionalized SWCNTs. This effect is sensitive to the laser energy that must be in resonance with the nanoparticle plasmon, and it was more pronouncedly observed using the 1.96 eV laser energy. It is well known that the enhancement factors in SERS are much larger

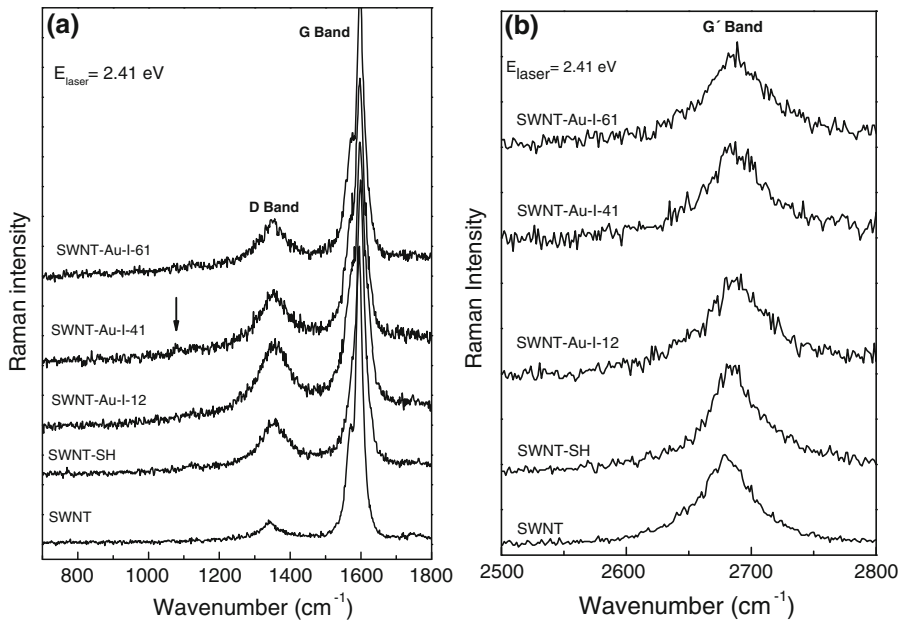

Fig. 7 Raman spectra in the **a** D- and G-band and **b** G′-band regions for SWCNT, SWCNT-SH, SWCNT-Au-I, using 2.41 eV as excitation energy

when the nanoparticles are adjacent, the distance between the particles being smaller than 2.5 times the particle diameter (Chu et al. 2009). By increasing the density of AuNP on the nanotube surface, i.e., increasing the Au:SWCNT ratio, an increase in the Raman enhancement of the thiol modes is expected. Indeed, this is observed in Fig. 6 for AuNP-loaded SWCNT prepared with both in situ and *ex situ* conditions. The absence of the peaks related to S–H bond vibrations suggests the interaction of the AuNPs with the nanotubes through the dithiol molecules of the S terminal groups. Although the surface plasmon absorption band of the AuNPs in suspension was observed at 535 nm before interacting with carbon nanotubes, the SERS effect using 2.41 eV (532 nm) is not so pronounced as the enhancement effect observed using 1.96 eV (632 nm) excitation energy. This behavior can be explained because after the interaction with the carbon nanotubes through the thiol molecules, the nanoparticles get closer to each other, thus causing a red-shift in the plasmon absorption band energy (Sendroiu et al. 2006).

Figure 8a and b depicts the TEM image of Au-SWCNT-S-I-41 (obtained by the in situ method), and Au-SWCNT-S-E-41 (obtained by the *ex situ* method) samples, respectively. The Au-SWCNT-S-I-41 (Fig. 8a) image show irregular sized AuNP, thus suggesting their coalescence on the surface of the SWCNTs bundles during reduction reaction. Figure 8b of Au-SWCNT-S-E-41 shows a bundle of SWCNT-SH highly covered by AuNPs. Moreover, it can be seen a small uncovered portion of the SWCNTs bundle, which allows us to infer that the AuNPs in this case is thicker and denser than that obtained by in situ method.

By comparing the samples having different ratio of Au:thiol (not shown here), it was observed that the quantity of $[AuCl_4]^-$ initially added to the reaction did not influence the size distribution of the NPs but did influence on the amount and density of AuNPs loading on the SWCNTs surface. The enhancement of the Raman signals supports the assumptions that the intermediate coverage fulfills the interparticle distance to particle size ratio conditions that are responsible for the highest surface enhancement Raman effect. Therefore, the enhancement is not effective neither for low-density coverage nor for very high-density coverage.

Figure 8c–f shows the image and elemental mapping of C, Au, and S of a SWCNT-SH bundle covered by AuNPs (Au-SWCNT-S-E-41 sample). These mapping allow us to confirm the functionalization of the carbon nanotubes by the presence of the S all over the nanotube bundle (Fig. 8f), responsible for the good interaction with and highly loading of Au on it (Fig. 8e).

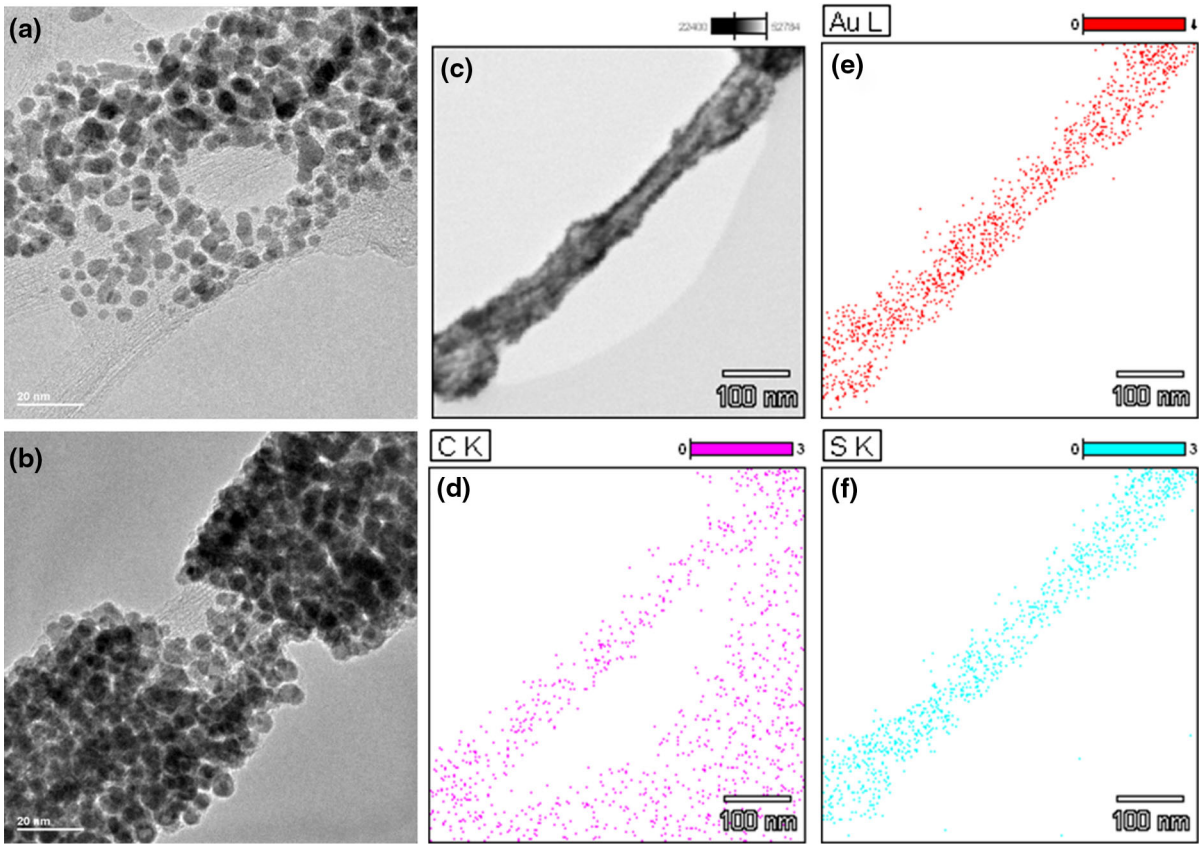

Fig. 8 TEM images of **a** Au-SWCNT-S-I-41 and **b** Au-SWCNT-S-E-41. **c** Elemental mapping images for Au-SWCNT-S-E-41 sample: **d** C, **e** Au and **f** S mapping

The average diameter of the AuNPs measured from the TEM images was about 4 nm for both samples, but the coverage of the carbon nanotube bundles is drastically different. As can be observed, the in situ method lead to an irregular and poor coverage, while the *ex situ* method resulted in a highly dense loading of AuNPs on the SWCNT-SH bundle. Due to this, the enhancement of thiol peaks in the Raman spectra was observed to be obtained at a lower concentration for the samples prepared by the *ex situ* method than for the sample prepared by the in situ method.

Conclusions

In summary, we have successfully prepared a hybrid system which consist of gold nanoparticles anchored to single wall carbon nanotube surface through the 4,4′-thiobisbenzenethiol molecule. These systems were prepared using both in situ and *ex situ* methodologies, and the results indicate that both methodologies can be efficiently used for decorating carbon nanotubes with gold nanoparticles. We have demonstrated the role of the 4,4′-thiobisbenzenethiol functionalization on the gold nanoparticle size distribution and their density on the nanotube surface. Transmission electron microscope images revealed that carbon nanotubes are covered with a high and uniform density of gold nanoparticles. Resonance Raman spectroscopy data revealed that charge transfer process between carbon nanotubes and gold nanoparticles are mediated by the thiol molecule. The anchoring of gold nanoparticles to the nanotube through 4,4′-thiobisbenzenethiol molecule is confirmed by observing the surface enhancement Raman effect which allowed us to access the Raman signal of thiol. Changes in the Raman signal of 4,4′-thiobisbenzenethiol are discussed in terms of nanoparticle density and the resonance with surface plasmon. Such hybrid systems may be suitable for applications, which

demand a high density of stabilized and immobilized gold nanoparticles covering the nanotubes. In addition, since the linker between carbon nanotubes and gold nanoparticles is a delocalized π-system, small changes occurring at the surface of the gold nanoparticles can be tracked by monitoring the very sensitive electronic structure of the carbon nanotubes, so that the nanotubes are used not only as support for the nanoparticles but also as active-building block when integrated in analytical and sensing devices.

Acknowledgments The authors acknowledge the LEM/LNLS (Electron Microscopy Laboratory/Brazilian Synchrotron Light Laboratory, Campinas) for the use of the microscope, the financial support from the Brazilian agencies CNPq (Conselho Nacional de Desenvolvimento Científico e Tecnlógico), CAPES, (Coordenação de Aperfeiçoamento de Pessoal de Nível Superior), and FAPESP (Fundação de Amparo à Pesquisa do Estado de São Paulo) and prof. C. Collins for the critical reading of the manuscript. AGSF acknowledge the Visiting Research Grant 08/58194-7 from FAPESP. This is a contribution of the INOMAT and NanoBioSimes National Institutes (MCTI-CNPq). AGSF and OPF acknowledge funding from PRONEX–FUNCAP.

References

Balasubramanian K, Burghard M (2005) Chemically functionalized carbon nanotubes. Small 1:180–192. doi:10.1002/smll.200400118

Chen Y-C, Young RJ, Macpherson JV, Wilson NR (2007) Single-walled carbon nanotube networks decorated with silver nanoparticles: a novel graded SERS substrate. J Phys Chem C 111:16167–16173. doi:10.1021/jp073771z

Chu H, Wang J, Ding L et al (2009) Decoration of gold nanoparticles on surface-grown single-walled carbon nanotubes for detection of every nanotube by surface-enhanced Raman spectroscopy. J Am Chem Soc 131:14310–14316. doi:10.1021/ja9035972

Costa S, Scheibe B, Rummeli M, Borowiak-Palen E (2009) Raman spectroscopy study on concentrated acid treated carbon nanotubes. Phys Status Solidi 246:2717–2720. doi:10.1002/pssb.200982297

de Souza Filho AG, Fagan SB (2007) Functionalization of carbon nanotubes. Quim Nov 30:1695–1703. doi:10.1590/S0100-40422007000700037

Ellis AV, Vijayamohanan K, Goswami R et al (2003) Hydrophobic anchoring of monolayer-protected gold nanoclusters to carbon nanotubes. Nano Lett 3:279–282. doi:10.1021/nl025824o

Fagan SB, Filho AGS, Filho JM et al (2005) Electronic properties of Ag- and CrO3-filled single-wall carbon nanotubes. Chem Phys Lett 406:54–59. doi:10.1016/j.cplett.2005.02.091

Farhat H, Son H, Samsonidze GG et al (2007) Phonon softening in individual metallic carbon nanotubes due to the Kohn anomaly. Phys Rev Lett 99:145506. doi:10.1103/PhysRevLett.99.145506

Furtado CA, Kim UJ, Gutierrez HR et al (2004) Debundling and dissolution of single-walled carbon nanotubes in amide solvents. J Am Chem Soc 126:6095–6105. doi:10.1021/ja039588a

Hirsch A (2002) Functionalization of single-walled carbon nanotubes. Angew Chem Int Ed 41:1853–1859. doi:10.1002/1521-3773(20020603)41:11<1853:AID-ANIE1853>3.0.CO;2-N

Hou X, Wang L, Zhou F, Wang F (2009) High-density attachment of gold nanoparticles on functionalized multiwalled carbon nanotubes using ion exchange. Carbon N Y 47:1209–1213. doi:10.1016/j.carbon.2008.12.004

Hu J, Shi J, Li S et al (2005) Efficient method to functionalize carbon nanotubes with thiol groups and fabricate gold nanocomposites. Chem Phys Lett 401:352–356. doi:10.1016/j.cplett.2004.11.075

Jiang L, Gao L (2003) Modified carbon nanotubes: an effective way to selective attachment of gold nanoparticles. Carbon N Y 41:2923–2929. doi:10.1016/S0008-6223(03)00339-7

Jiang K, Eitan A, Schadler LS et al (2003) Selective attachment of gold nanoparticles to nitrogen-doped carbon nanotubes. Nano Lett 3:275–277. doi:10.1021/nl025914t

Kauffman DR, Star A (2007) Chemically induced potential barriers at the carbon nanotube–metal nanoparticle interface. Nano Lett 7:1863–1868. doi:10.1021/nl070330i

Kauffman DR, Sorescu DC, Schofield DP et al (2010) Understanding the sensor response of metal-decorated carbon nanotubes. Nano Lett 10:958–963. doi:10.1021/nl903888c

Kim YT, Mitani T (2006) Surface thiolation of carbon nanotubes as supports: a promising route for the high dispersion of Pt nanoparticles for electrocatalysts. J Catal 238:394–401. doi:10.1016/j.jcat.2005.12.020

Kim UJ, Furtado CA, Liu X et al (2005) Raman and IR spectroscopy of chemically processed single-walled carbon nanotubes. J Am Chem Soc 127:15437–15445. doi:10.1021/ja052951o

Kim Y-T, Uruga T, Mitani T (2006) Formation of single Pt atoms on thiolated carbon nanotubes using a moderate and large-scale chemical approach. Adv Mater 18:2634–2638. doi:10.1002/adma.200502019

Kneipp K, Kneipp H, Itzkan I et al (1999) Ultrasensitive chemical analysis by Raman spectroscopy. Chem Rev 99:2957–2976. doi:10.1021/cr980133r

Kumar S, Kaur I, Dharamvir K, Bharadwaj LM (2012) Controlling the density and site of attachment of gold nanoparticles onto the surface of carbon nanotubes. J Colloid Interface Sci 369:23–27. doi:10.1016/j.jcis.2011.11.045

Li D, Zhang Y, Jiang J, Li J (2003) Electroactive gold nanoparticles protected by 4-ferrocene thiophenol monolayer. J Colloid Interface Sci 264:109–113. doi:10.1016/S0021-9797(03)00373-4

Li J, Huang Y, Chen P, Chan-Park MB (2013) In situ charge-transfer-induced transition from metallic to semiconducting single-walled carbon nanotubes. Chem Mater 25:4464–4470. doi:10.1021/cm401040d

Lim JK, Yun WS, Yoon M et al (2003) Selective thiolation of single-walled carbon nanotubes. Synth Met 139:521–527. doi:10.1016/S0379-6779(03)00337-0

Liu HW, Bhushan B, Eck W, Stadler V (2001) Investigation of the adhesion, friction, and wear properties of biphenyl thiol self-assembled monolayers by atomic force microscopy. J Vac Sci Technol, A 19:1234–1240. doi:10.1116/1.1353538

Liu L, Wang TX, Li JX et al (2003) Self-assembly of gold nanoparticles to carbon nanotubes using a thiol-terminated pyrene as interlinker. Chem Phys Lett 367:747–752. doi:10.1016/S0009-2614(02)01789-X

Liz-Marzán LM (2004) Nanometals: formation and color. Mater Today 7:26–31. doi:10.1016/S1369-7021(04)00080-X

Maciel IO, Anderson N, Pimenta MA et al (2008) Electron and phonon renormalization near charged defects in carbon nanotubes. Nat Mater 7:878–883. doi:10.1038/nmat2296

Mubeen S, Zhang T, Yoo B et al (2007) Palladium nanoparticles decorated single-walled carbon nanotube hydrogen sensor. J Phys Chem C 111:6321–6327. doi:10.1021/jp067716m

Ou Y–Y, Huang MH (2006) High-density assembly of gold nanoparticles on multiwalled carbon nanotubes using 1-pyrenemethylamine as interlinker. J Phys Chem B 110:2031–2036. doi:10.1021/jp055920o

Peng H, Alemany LB, Margrave JL, Khabashesku VN (2003) Sidewall carboxylic acid functionalization of single-walled carbon nanotubes. J Am Chem Soc 125:15174–15182. doi:10.1021/ja037746s

Raghuveer MS, Agrawal S, Bishop N, Ramanath G (2006) Microwave-assisted single-step functionalization and in situ derivatization of carbon nanotubes with gold nanoparticles. Chem Mater 18:1390–1393. doi:10.1021/cm051911g

Ramanathan T, Fisher FT, Ruoff RS, Brinson LC (2005) Amino-functionalized carbon nanotubes for binding to polymers and biological systems. Chem Mater 17:1290–1295. doi:10.1021/cm048357f

Scolari M, Mews A, Fu N et al (2008) Surface enhanced Raman scattering of carbon nanotubes decorated by individual fluorescent gold particles. J Phys Chem C 112:391–396. doi:10.1021/jp076190i

Sendroiu IE, Mertens SFL, Schiffrin DJ (2006) Plasmon interactions between gold nanoparticles in aqueous solution with controlled spatial separation. Phys Chem Chem Phys 8:1430–1436. doi:10.1039/B518112G

Srivastava SK, Yamada R, Ogino C, Kondo A (2013) Sidewall modification of multiwalled carbon nanotubes by *Allium sativum* (garlic) and its effect on the deposition of gold nanoparticles. Carbon N Y 56:309–316. doi:10.1016/j.carbon.2013.01.021

Star A, Joshi V, Skarupo S et al (2006) Gas sensor array based on metal-decorated carbon nanotubes. J Phys Chem B 110:21014–21020. doi:10.1021/jp064371z

Suni II (2008) Impedance methods for electrochemical sensors using nanomaterials. TrAC-Trends Anal Chem 27:604–611. doi:10.1016/j.trac.2008.03.012

Voggu R, Pal S, Pati SK, Rao CNR (2008) Semiconductor to metal transition in SWNTs caused by interaction with gold and platinum nanoparticles. J Phys Condens Matter. doi:10.1088/0953-8984/20/21/215211

Wang Y, Gan L, Chen H et al (2006) Structure and identity of 4,4‘-thiobisbenzenethiol self-assembled monolayers. J Phys Chem B 110:20418–20425. doi:10.1021/jp062422m

Wang Y, Chen H, Dong S, Wang E (2008) Adsorption of 4,4′-thiobisbenzenethiol on silver surfaces: surface-enhanced Raman scattering study. J Raman Spec 39:389–394. doi:10.1002/jrs.1836

Weckenmann U, Mittler S, Naumann K, Fischer RA (2002) Ordered self-assembled monolayers of 4,4′-biphenyldithiol on polycrystalline silver: suppression of multilayer formation by addition of tri-*n*-butylphosphine. Langmuir 18:5479–5486. doi:10.1021/la011857s

Wu B, Hu D, Kuang Y et al (2009) Functionalization of carbon nanotubes by an ionic-liquid polymer: dispersion of Pt and PtRu nanoparticles on carbon nanotubes and their electrocatalytic oxidation of methanol. Angew Chem Int Ed 48:4751–4754. doi:10.1002/anie.200900899

Zanella R, Sandoval A, Santiago P et al (2006) New preparation method of gold nanoparticles on SiO_2. J Phys Chem B 110:8559–8565. doi:10.1021/jp060601y

Zhang R, Hummelgard M, Olin H (2009) Simple and efficient gold nanoparticles deposition on carbon nanotubes with controllable particle sizes. Mater Sci Eng, B 158:48–52. doi:10.1016/j.mseb.2008.12.038

Zhao L, Shingaya Y, Tomimoto H et al (2008) Functionalized carbon nanotubes for pH sensors based on SERS. J Mater Chem 18:4759–4761. doi:10.1039/B809833F

Zhu H, Lu X, Li M et al (2009) Nonenzymatic glucose voltammetric sensor based on gold nanoparticles/carbon nanotubes/ionic liquid nanocomposite. Talanta 79:1446–1453. doi:10.1016/j.talanta.2009.06.010